

## Epitactic textures of fcc Al on icosahedral Al-Pd-Mn quasicrystal

B. Bolliger, V. E. Dmitrienko,\* M. Erbudak, R. Lüscher, and H.-U. Nissen  
*Laboratorium für Festkörperphysik, ETH Zürich, CH-8093 Zürich, Switzerland*

A. R. Kortan

*Bell Laboratories, Lucent Technologies, Murray Hill, New Jersey 07974*

(Received 24 August 2000; published 12 January 2001)

An aluminum film is deposited on the fivefold-symmetric surface of icosahedral Al-Pd-Mn quasicrystal. Its orientation with respect to the bulk structure is studied using low-energy electron diffraction. It is found that Al nanocrystals grow in the face-centered cubic structure in five different sets of domains composing the film, and that their [111] axes are aligned parallel to one of five threefold-symmetry axes of the substrate quasicrystal at  $37.37^\circ$  away from the surface normal.

DOI: 10.1103/PhysRevB.63.052203

PACS number(s): 61.44.Br, 61.14.-x, 68.35.Bs

In contrast to crystals, quasicrystals (QC's) are characterized by their lack of long-range periodic atomic order. This basic difference in the type of order between the two classes of solids makes it impossible that crystals grown on QC's and *vice versa* have a long-range commensurability of their lattice respectively quasilattice. It is important to establish the geometric relationship crystal to quasicrystal at their mutual interface, because in several industrial applications QC's are used as a thin coating on conventional crystalline material.<sup>1</sup> Also, the knowledge of the precise geometrical relationship between the two types of materials at their boundary offers additional crystal-chemical information on the QC's. Numerous observations indicate that the quasicrystalline and related crystalline structures can coexist with a limited number of definite orientational relationships.<sup>2</sup> Commonly, the associated crystalline structures are so-called approximants, i.e., crystals that contain regions with the same local atomic ordering scheme as exists in the related QC's. The simplest approximant for the present case is AlPd in the B2 structure that can grow on surfaces of quasicrystalline Al-Pd-Mn.<sup>3-5</sup>

QC's are stable only in a limited region of their phase diagram so that small changes in the chemical composition can induce a phase transformation. A depletion of Al at the surface induced by preferential removal under ion bombardment changes the near-surface region into material with the B2 crystal structure. This cubic phase was found to grow in a specific orientation relation with the underlying icosahedral (*i*-) QC.<sup>3-5</sup> In this case a twofold-symmetry axis of the cube is aligned along a fivefold-symmetry axis of the QC, and one threefold axis of the approximant nearly coincides with one threefold axis of the icosahedron.<sup>3,6</sup> However, this surface layer was found to be unstable; it reverts to its original chemical composition and to the icosahedral structure as a result either of annealing-induced surface segregation of Al at  $400^\circ\text{C}$  or as a result of a mild annealing up to  $150^\circ\text{C}$  after vacuum deposition of Al onto the sample surface. On the other hand, if the Al concentration in the near-surface region is too high, the QC is not in the stable region of the phase diagram any more.

Here, we report the growth of cubic Al on the pentagonal surface of *i*-Al<sub>70</sub>Pd<sub>20</sub>Mn<sub>10</sub> QC. It was essential to maintain

the surface temperature below  $50^\circ\text{C}$  during deposition of Al, in order to prevent diffusion of Al into the sample. A continuous (of Frank-van der Merve type) growth was aimed at by setting the ratio between the evaporation rate and the surface temperature below a certain value.<sup>7</sup> These considerations allow the deposition rate of Al on Al-Pd-Mn to be controlled by the temperature of the indirectly heated Al atom source. It was found that the film consisted of domains with five distinct orientations of face-centered-cubic (fcc) material. Their orientations are determined by the substrate as follows: The [111] axes of the fcc single-crystal domains are aligned parallel to one of the five threefold-symmetry directions that are located on a cone with a polar angle of  $\theta=37.37^\circ$  away from the surface normal corresponding to one pentagonal direction of the icosahedron.

The single-grain Al<sub>70</sub>Pd<sub>20</sub>Mn<sub>10</sub> sample used in the present experiments was grown by conventional techniques<sup>8</sup> and was subsequently oriented along one of its pentagonal axes, with an accuracy of  $\pm 0.5^\circ$ , by the x-ray Laue method. It was then cut by spark erosion into the shape of a cylinder having a diameter of approximately 8 mm and a thickness of 2 mm. Its surface was polished by applying diamond pastes with different grain sizes down to a coarseness of  $0.3\ \mu\text{m}$ , before the specimen was inserted into vacuum. It was mounted onto a holder incorporating a resistance-heated oven, and the temperature was measured with a chromel-alumel thermocouple that was in contact with the surface. The surface of the sample was then cleaned in vacuum by sputtering with Ar<sup>+</sup> ions at 1500 eV and a current density of  $5 \times 10^{-7}\ \text{A}/\text{mm}^2$  for 20 min. Afterward it was heat treated at 700 K, typically for 30 min, followed by a brief flashing at 900 K. The surface structure was observed by secondary-electron imaging (SEI)<sup>3</sup> and low-energy electron diffraction (LEED). The chemical composition at the surface was determined using Auger electron spectroscopy. The data were calibrated by comparative measurements on clean Al and Pd metal surfaces. It was found that within error limits of  $\pm 1\%$  the chemical composition at the surface was the same as that in the bulk. The evaporation rate of Al was  $2.5\ \text{\AA}/\text{min}$ , determined by recording Al (72 eV) and Cu (920 eV) Auger signals during growth of Al on Cu and using 5 and  $10\ \text{\AA}$  for the mean-free path of electrons, respectively. The pressure in the experimental

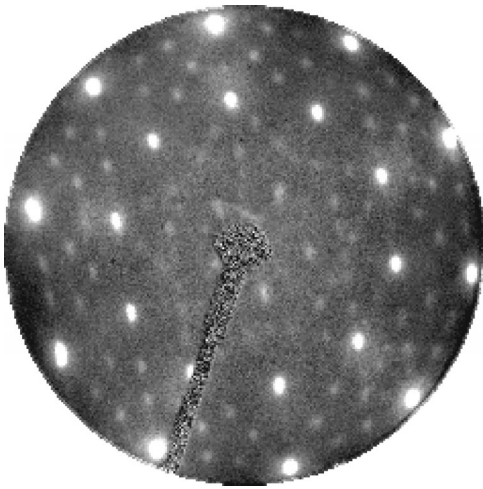


FIG. 1. LEED pattern obtained from the fivefold-symmetric surface of  $\text{Al}_{70}\text{Pd}_{20}\text{Mn}_{10}$  *i*-QC at a primary-electron energy of 72 eV. Details of variations in the spot-intensity reveal that the distribution of atoms on the analyzed volume is fivefold symmetric.

chamber remained in the  $10^{-9}$ -Pa range during Al evaporation.

Figure 1 shows a LEED pattern of a well-ordered fivefold plane of the *i*-QC sample. This corresponds to the structure of a surface layer of approximately 5–8-Å thickness, normal to a fivefold axis. The thickness of this layer was determined by the mean-free path of the primary electrons at an energy of 72 eV. The orientation of the sample was such that the fivefold-symmetry axis was parallel to the direction of primary-electron incidence, i.e., the display center. As the electron energy was increased, the spots converged toward the display center, where the specular reflection was concealed behind the elongate shadow of the electron gun. The resulting pattern is almost tenfold symmetric. The overall fivefold symmetry of the pattern is only revealed by certain details of the spots, e.g., by an uneven distribution of spot intensities. The quality of the pattern confirms the presence of a bulk-terminated surface.<sup>9,10</sup>

After vacuum deposition of approximately 5 Å of Al, the LEED pattern observed on the screen drastically changed in a continuous manner up to a layer thickness of approximately 15 Å. Figure 2 displays the LEED patterns taken after evaporating a 20-Å-thick layer of Al on the cleaned, quasicrystalline, fivefold-symmetric surface at primary-electron energies of 63 and 66 eV, respectively. The specimen here has the same orientation as in Fig. 1. The new LEED patterns display a more pronounced fivefold symmetry than that observed from a quasicrystalline structure (cf. Fig. 1), for which the spot distribution with an odd-numbered symmetry is entirely due to multiple scattering. Apparently, the analyzed surface layer consists of a texture of domains in five different orientations. This becomes evident from the changes in position of the spots on the hemispheric screen that occur when the energy of the primary-electron beam is varied. Each of the observed positions of a specular reflection is surrounded by a symmetric arrangement of bright spots corresponding to the LEED pattern of a single crystal. The small difference of 3 eV in the primary energy results in

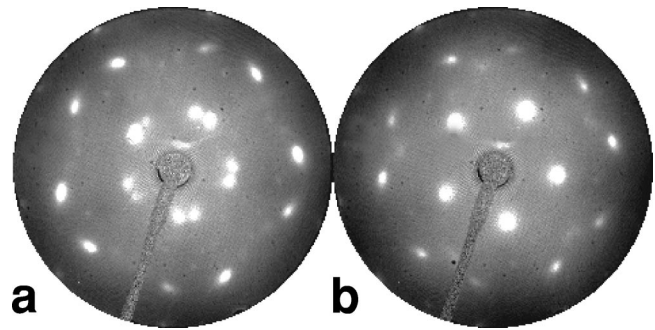


FIG. 2. LEED patterns obtained from the fivefold-symmetric surface of  $\text{Al}_{70}\text{Pd}_{20}\text{Mn}_{10}$  *i*-QC at primary-electron energies of (a) 63 eV and (b) 66 eV, after evaporating a 20-Å-thick layer of Al. The fivefold symmetry of the patterns is consistent with a growth mode of Al in domains with five different orientations.

a considerable change in the position of the spots on the spherical collector screen confirming that they are high-angle diffraction spots. For the given position of the sample, i.e., for approximately normal incidence of the primary-electron beam, the specular beam must have a large angular distance from the surface normal.

In order to determine the orientation of each of the five individual specular beams, the specimen was rotated in different experiments around a polar as well as an azimuthal axis. If during these experiments the primary beam was incident on the specimen surface approximately parallel to one of the threefold-symmetry axes of the QC substrate, then the specular beam that was reflected from an Al crystal domain coincided with the primary beam and thus with the display axis. Using this procedure, we found that each domain was inclined by approximately  $37^\circ$  with respect to the pentagonal axis of the substrate, and the domains were distributed in equal azimuthal increments around the macroscopic surface normal.

The LEED spot pattern for one case of such an alignment is presented in Fig. 3(a). A schematic representation of the reflections occurring in this pattern is given in Fig. 3(b). To the left of the shadow of the electron gun a bright spot

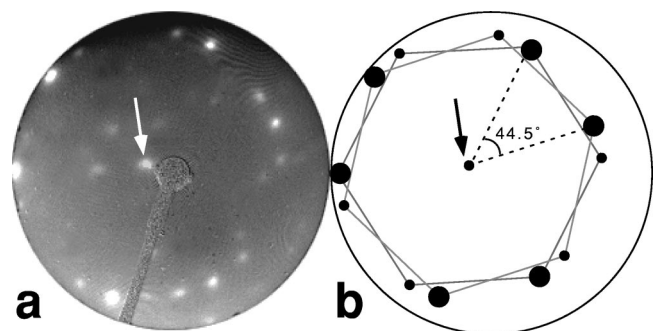


FIG. 3. (a) LEED pattern obtained from the Al film after rotating the sample by approximately  $37^\circ$  such that a threefold-symmetry axis of the QC substrate is now almost parallel to the direction of primary-electron incidence. The specularly reflected beam is marked by an arrow. (b) Two hexagons centered around the specular beam mark the distribution of diffracted beams from two domains sharing the same [111] axis.

marked by an arrow corresponds to the specular (00) beam of one crystallite orientation. When the electron energy is varied, the position of this spot remains constant. This is evidence that the bright spot corresponds to the (00) beam. While the primary energy is increased, the spots distributed near the rim of the screen converge toward the (00) spot. The observed spots consist of two sets of six reflections each. In Fig. 3(b) these two sets are marked by lines connecting the reflections. In each of these two sets three reflections are brighter than the other three. This indicates the threefold symmetry of a (111) surface for a cubic crystal. The second set is rotated against the first one by approximately  $45^\circ$ ; this indicates the presence of two distinct orientation relations of Al crystallites having the same [111] axis parallel to the threefold-symmetry axis of the quasicrystal matrix. The distribution of these spots corresponds to a cubic lattice parameter of approximately  $4.05 \text{ \AA}$ , characteristic of the Al single crystal. The spots observed in addition to these originate from other domains. When the specimen is rotated from the orientation of the (00) beam parallel to one threefold-symmetry axis into a position parallel to another threefold axis of the icosahedral system, a pattern with an analogous arrangement of bright spots results. The sum of all the superimposed LEED patterns indicates that in the Al layer resting on the quasicrystal substrate five different orientations of the [111] directions of Al crystallites coexist. We therefore conjecture that the small regions of the surface of the Al film are not parallel to the substrate surface but grown as surfaces of small octahedra oriented perpendicular to the threefold-symmetry axes of the icosahedron.

The SEI patterns obtained from the specimen containing the evaporated film of  $20\text{-\AA}$  thickness were identical to those from the bare substrate.<sup>3</sup> For successful imaging by the SEI technique, a homogeneous local order inside the analyzed volume of the specimen is required. The resulting SEI pattern must be interpreted as an average structure of the analyzed volume of material. This is consistent with our present LEED observations, since the observed fivefold-symmetric pattern is explained as the average SEI pattern from the five differently oriented sets of Al domains with their [111] directions aligned along the icosahedral threefold-symmetry axes. Thus, the fine structure of the domain texture could be revealed by the diffraction experiment. An upper and a lower limit of the domain size can be obtained from the LEED observations. The electron beam has a diameter of  $0.3 \text{ mm}$ . Hence, the ensemble of the domains must be smaller than this dimension, so that each set of equally oriented domains makes an approximately equal contribution to the observed pattern. Each domain produces a distinct LEED pattern without an interference between the domains having different orientations. This indicates that each domain scatters independently from others possibly because the domains are distributed on the surface quasiperiodically, i.e., incommensurately with their cubic periodicity. Using the spot-intensity profiles we can estimate the domains as large as  $50\text{--}100 \text{ \AA}$ . The observed domain texture of the Al film was found to be identical for films as thick as  $80 \text{ \AA}$ .

The available previous experimental information on the annealed fivefold quasicrystalline surface structure of

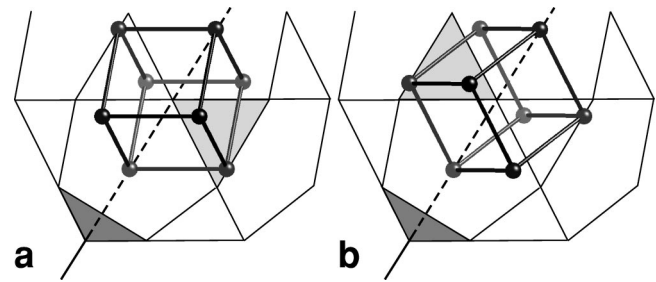


FIG. 4. Scheme of an icosidodecahedron surrounding a cube in two different orientations, rotated against each other around a common [111] axis (dashed line) by  $44.48^\circ$ . The crystallite domains in the experiment are rotated against each other by the same angle. The dashed line passes through the center of the dark-shadowed triangular facet whereas another threefold axis of the cube passes through the center of the light-shadowed triangle.

*i*-Al-Pd-Mn is controversial. Depending on the surface treatment, either a stepped surface<sup>9,11</sup> or a puckered surface covered with atomic clusters is obtained.<sup>12</sup> In both cases no experimental information on the atomic arrangement at the surface has hitherto been obtained. In order to gain insight into the growth mechanism of Al on the *i*-QC surface, the atomic-scale surface structure of the QC without the subsequently evaporated Al was simulated by a Monte Carlo calculation. It is based on an algorithm for the simulation of crystal growth.<sup>13</sup> Modified for the application to *i*-QC's, it allows the investigation of the growth and melting process at the surface.<sup>14,15</sup> The Katz-Gratias model<sup>16</sup> of the *i*-QC was used as an initial structure for modeling the process of annealing by the Monte Carlo calculations. The difference between Al, Pd, and Mn was ignored. Nevertheless, this model can be regarded as sufficiently realistic since it incorporates interatomic bonds known from the x-ray and neutron-scattering investigations,<sup>17</sup> and it contains motives of local order observed in several crystalline approximants.<sup>18</sup> We are aware of the fact that the structure of the bare QC surface may change upon Al evaporation. However, we could not observe any changes in the original LEED patterns (cf. Fig. 1) up to approximately the  $5\text{-\AA}$ -thick Al layer. The details of the Monte Carlo simulation will be communicated later.

The Monte Carlo simulation results in an undulated surface with depressions that have the shape of an incomplete icosidodecahedron. Atoms are at the vertices of the icosidodecahedron and near the center of pentagonal facets, forming the outer shell of the Mackay icosahedron. According to Fig. 4 there are two equivalent orientations of a cube with respect to the fixed orientation of an icosidodecahedron, for which the threefold-symmetry axes of both polyhedra are parallel. The angular displacement around a [111] axis is  $\cos^{-1}(\tau^2+2)/4\tau=44.48^\circ$ , with  $\tau=(1+\sqrt{5})/2$ . This different relative arrangement of the symmetry axes of the  $(m\bar{3}m)$  and the  $(\bar{5}\bar{3}m)$  point group is found to be different from the orientation of a surface layer in the bcc structure obtained through sputtering the *i*-QC.<sup>3,6</sup> In this arrangement there are common symmetry elements belonging to the point group  $(m\bar{3})$ , which is therefore the subgroup common to both structures.<sup>14</sup>

The Monte Carlo simulations allow the assumption that the concave depletions are suitable places for initial seeds of fcc Al crystals that are coherently oriented relative to the quasicrystal matrix. An indirect confirmation of this hypothesis may be found in the structure of the crystalline approximants. Indeed, in the approximants, the *B2*-type cubic arrangements of 15 atoms were observed rather frequently inside the outer shell of the Mackay icosahedra, for example, in the crystalline alloys  $\text{Al}_{68}\text{Pd}_{20}\text{Ru}_{12}$  (Ref. 19) and  $\text{Al}_{39}\text{Fe}_3\text{Pd}_2$ ,<sup>20</sup> which are the 1/0 approximants of the corresponding *i*-QC, and in  $\text{Al}_{70}\text{Pd}_{23}\text{Mn}_6\text{Si}$ ,<sup>21</sup> which is the 2/1 approximant of that structure. These 15 atoms are positioned as follows: one atom at the center of the cube formed by eight atoms and remaining six atoms at fourfold cubic directions. An fcc arrangement was never encountered before; however, in the approximants  $\text{Mg}_2\text{Zn}_{11}$  (Ref. 22) and  $\text{Al}_5\text{Cu}_6\text{Mg}_2$  (Ref. 23) the atomic arrangement has been found to be very close to fcc. It is similar to the *B2*-type cluster, except that the center atom is absent and six atoms

are very near the face centers. This cluster of 14 atoms forms a structure similar to the fcc-based  $\text{AuCu}_3$  alloy, and clusters of this type may be a seed for further growth of Al fcc crystals, as possibly in the present experimental case. At present, it appears difficult to prove our assumption. We should emphasize, however, that the interpretation of our experimental results is independent of this hypothesis.

In evaluating the present results of the Al growth on the quasicrystalline substrate it is also of interest that the periodic average structure of the three-dimensional Ammann tiling of *i*-QC is very similar to the fcc lattice of Al.<sup>24</sup> Therefore, one can expect a long-range coincidence between fcc Al and *i*-QC. This average structure can have precisely those five different orientations of its domains with respect to the *i*-QC that are shown here to be present for Al in the LEED experiments.

V.E.D. acknowledges the hospitality and financial support of ETH Zürich. Partial funding was provided for this work by Schweizerischer Nationalfonds.

\*Permanent address: Institute of Crystallography, 59 Leninski prospect, Moscow, 117333, Russia.

<sup>1</sup>J. M. Dubois, in *New Horizons in Quasicrystals*, edited by A. I. Goldman *et al.* (World Scientific, Singapore, 1997).

<sup>2</sup>A. Loiseau and G. Lapasset, *J. Phys. (Paris), Colloq.* **47**, C-3, 331 (1986); C. Beeli, *Z. Kristallogr.* **215**, 606 (2000).

<sup>3</sup>B. Bolliger, M. Erbudak, D. D. Vvedensky, M. Zurkirch, and A. R. Kortan, *Phys. Rev. Lett.* **80**, 5369 (1998).

<sup>4</sup>Z. Shen *et al.*, *Phys. Rev. B* **58**, 9961 (1998).

<sup>5</sup>D. Naumović *et al.*, *Phys. Rev. B* **60**, R16 330 (1999).

<sup>6</sup>B. Bolliger, M. Erbudak, A. Hensch, and D. D. Vvedensky, *Mater. Sci. Eng., A* (to be published).

<sup>7</sup>*Epitaxial Growth*, Part B, edited by J. W. Matthews (Academic Press, New York, 1975).

<sup>8</sup>A. R. Kortan *et al.*, *Phys. Rev. B* **40**, 9397 (1989).

<sup>9</sup>T. M. Schaub, D. E. Bürgler, H.-J. Güntherodt, and J.-B. Suck, *Phys. Rev. Lett.* **73**, 1255 (1994).

<sup>10</sup>M. Gierer *et al.*, *Phys. Rev. Lett.* **78**, 467 (1997); M. Gierer *et al.*, *Phys. Rev. B* **57**, 7628 (1998).

<sup>11</sup>B. Bolliger *et al.*, *Ferroelectrics* (to be published).

<sup>12</sup>P. Ebert, F. Yue, and K. Urban, *Phys. Rev. B* **57**, 2821 (1998).

<sup>13</sup>A. C. Levi and M. Kotrla, *J. Phys.: Condens. Matter* **9**, 299

(1997).

<sup>14</sup>V. E. Dmitrienko and S. B. Astaf'ev, *Phys. Rev. Lett.* **75**, 1538 (1995); *JETP Lett.* **61**, 331 (1995).

<sup>15</sup>V. E. Dmitrienko, S. B. Astaf'ev, and M. Kléman, *Phys. Rev. B* **59**, 286 (1999).

<sup>16</sup>A. Katz and D. Gratias, in *Lectures on Quasicrystals*, edited by F. Hippert and D. Gratias (Les Editions de Physique, Les Ulis, France, 1994), p. 187.

<sup>17</sup>M. Boudard *et al.*, *J. Phys.: Condens. Matter* **4**, 10 149 (1992).

<sup>18</sup>V. E. Dmitrienko, *Acta Crystallogr., Sect. A: Found. Crystallogr.* **50**, 515 (1994).

<sup>19</sup>S. Mahne and W. Steurer, *Z. Kristallogr.* **211**, 17 (1996).

<sup>20</sup>F. J. Edler, V. Gramlich, and W. Steurer, *J. Alloys Compd.* **269**, 7 (1998).

<sup>21</sup>K. Sugiyama, N. Kaji, and K. Hiraga, *Z. Kristallogr.* **213**, 90 (1998).

<sup>22</sup>T. Gödecke and F. Sommer, *Z. Metallkd.* **85**, 683 (1994).

<sup>23</sup>I. C. Barlow, W. M. Rainforth, and H. Jones, *J. Mater. Sci.* **35**, 1413 (2000).

<sup>24</sup>W. Steurer and T. Haibach, *Acta Crystallogr., Sect. A: Found. Crystallogr.* **55**, 48 (1999).